RSC Advances

PAPER

View Article Online
View Journal | View Issue

Cite this: *RSC Adv.*, 2023, **13**, 32928

Enhanced EDC removal from water through electron beam-mediated adsorber particle integration in microfiltration membranes†

Zahra Niavarani,[a] Daniel Breite,[a] Berfu Ulutaş,[ab] Andrea Prager,[a] Ömer Kantoğlu,[c] Bernd Abel,[d] Roger Gläser [d] and Agnes Schulze *[a]

The existence of endocrine disrupting chemicals (EDCs) in water and wastewater gives rise to significant environmental concerns. Conventional treatment approaches demonstrate limited capacity for EDC removal. Thus, incorporation of advanced separation procedures becomes essential to enhance the efficiency of EDC removal. In this work, adsorber composite microfiltration polyethersulfone membranes embedded with divinyl benzene polymer particles were created. These membranes were designed for effectively removing a variety of EDCs from water. The adsorber particles were synthesized using precipitation polymerization. Subsequently, they were integrated into the membrane scaffold through a phase inversion process. The technique of electron beam irradiation was applied for the covalent immobilization of particles within the membrane scaffold. Standard characterization procedures were carried out (*i.e.*, water permeance, contact angle, X-ray photoelectron spectroscopy and scanning electron microscopy) to gain a deep understanding of the synthesized membrane properties. Dynamic adsorption experiments demonstrated the excellent capability of the synthesized composite membranes to effectively remove EDCs from water. Particularly, among the various target molecules examined, testosterone stands out with the most remarkable enhancement, presenting an adsorption loading of 220 mg m^{-2}. This is an impressive 26-fold increase in the adsorption when compared to the performance of the pristine membrane. Similarly, androst-4-ene-3,17-dione exhibited an 18-fold improvement in adsorption capacity in comparison to the pristine membrane. The composite membranes also exhibited significant adsorption capacities for other key compounds, including 17β-estradiol, equilin, and bisphenol-A. With the implementation of an effective regeneration procedure, the composite membranes were put to use for adsorption over three consecutive cycles without any decline in their adsorption capacity.

Received 18th September 2023
Accepted 30th October 2023

DOI: 10.1039/d3ra06345c

rsc.li/rsc-advances

Introduction

The rising occurrence of endocrine disrupting chemicals (EDCs) in various water sources globally has emerged as a significant health concern for both humans and wildlife.[1,2] Existing research has demonstrated that exposure to EDCs, even at low concentrations (ng L^{-1} to μg L^{-1}), has been linked to various negative health outcomes, including reproductive and developmental problems, neurological damage, and an increased risk of various types of cancer.[3–5] Furthermore, EDCs impact the environment, contributing to population declines among aquatic organisms and ecosystem degradation.[6,7] The conventional methods of treating water and wastewater, including coagulation and flocculation, biological treatment, sorption onto polymers and resins, as well as chlorination and ozonation, while useful for many contaminants, fall short when it comes to the specific challenge of EDC removal. Despite their established utility for various pollutants, these methods have demonstrated limitations in addressing the unique properties and low concentrations of EDCs present in water sources.[8,9] Consequently, advanced treatment strategies are sought to address this deficiency and ensure the safeguarding of water quality. Various advanced water treatment techniques have been employed, including activated carbon adsorption and advanced oxidation.[10,11] However, each of these techniques has its own limitations. These limitations include the formation of potentially more toxic by-products and low removal efficiency.[12,13] Additionally, they involve demanding high-pressure and high-temperature conditions that necessitate significant

[a]*Leibniz Institute of Surface Engineering e.V. (IOM), Permoserstrasse 15, 04318 Leipzig, Germany. E-mail: agnes.schulze@iom-leipzig.de*
[b]*Department of Chemistry, Middle East Technical University, 06800 Ankara, Turkey*
[c]*TENMAK, Nuclear Energy Research Institute, Kahramankazan, 06980 Ankara, Turkey*
[d]*Institute of Chemical Technology, Universität Leipzig, Linnéstraße 3, 04103 Leipzig, Germany*

† Electronic supplementary information (ESI) available. See DOI: https://doi.org/10.1039/d3ra06345c

energy consumption.[14,15] Furthermore, these methods either lack a viable regeneration process or entail regeneration procedures that are excessively expensive and environmentally unsustainable.[16,17] Given the mentioned challenges, there is a pressing need for alternative approaches that are both sustainable and efficient in removing EDCs from water. While membrane processes, such as nanofiltration (NF) and reverse osmosis (RO), have shown promising results in removing EDCs from water, their dependency on high pressure and subsequent energy consumption renders them unsustainable in the long run.[18–20] In contrast to NF and RO, the application of polyethersulfone (PES) microfiltration (MF) membranes has shown significant potential for efficiently adsorbing EDCs from water. Notably, PES microfiltration membranes feature lower operating pressure requirements, leading to reduced energy consumption during the filtration process. The remarkable high porosity and robust hydrophilic properties of microfiltration PES membranes contribute to their efficacy in adsorbing EDC, given their extensive surface area for interaction. These characteristics make microfiltration PES membranes a viable and promising option for water treatment methods aiming to remove EDCs.[21] The utilization of composite membranes that incorporate adsorber particles has emerged as a highly effective approach for the removal of EDCs from water.[22,23] These adsorber particles, commonly composed of activated carbon, zeolite, or clay minerals, are uniformly dispersed within the membrane matrix using diverse techniques such as phase inversion, physical coating, interfacial polymerization, electrospinning, cross-linking, and chemical grafting. This integration facilitates an increased adsorption capacity and the selective removal of EDCs. This advanced technique presents a highly efficient water treatment method, demonstrating an adsorption capacity of 80% to 90% for a range of EDCs.[24–26] Through the application of this technique, the surface area of the membrane is notably increased, leading to a great enhancement in its capacity to adsorb EDCs. This augmented surface area allows for a greater contact between the membrane and the target contaminants, facilitating improved adsorption efficiency and overall performance in removing EDCs from water.[27–30] Incorporating adsorber particles into composite membranes adds customizable functionalities. These particles have a strong affinity for EDCs, efficiently attracting and adsorbing these contaminants through various interactions. Additionally, using composite membranes with adsorber particles decreases waste generation. These particles can be easily regenerated and reused, reducing the necessity for frequent module replacement.[31–33] This enhances sustainability and brings economic advantages by prolonging composite membrane lifespan and efficiency. Uebele *et al.*[22] implemented a wet spinning technique to synthesize mixed matrix membrane (MMM) adsorbers, utilizing three variations of anion exchange particles. Their study aimed to evaluate the effectiveness of this membrane system in simultaneously removing pharmaceuticals from water. The researchers reported that the MMM adsorbers exhibited notable adsorption capacities, with diclofenac being adsorbed at a rate of up to 13.7 g m^{-2} and sulfamethoxazole at a rate of up to 0.60 g m^{-2}. Similarly, Niedergall *et al.*[34] conducted a study focusing on the production of nanocomposite membrane adsorbers. In their research, selective nanospheres were integrated into PES membrane matrices using a wet-phase inversion process without cross-linking. The study revealed that the nanocomposite membranes had adsorption capacities up to 1.2 mg m^{-2} for bisphenol-A (BPA). Lotfi *et al.*[35] effectively immobilized TiO_2 nanoparticles onto both the surface and pores of a microfiltration PES membrane, leading to substantial photocatalytic degradation of 17β-estradiol (E2). In a solution with an initial concentration of 100 ng L^{-1}, a remarkable 94% degradation of E2 was achieved. Balta *et al.*[36] employed ZnO nanoparticles as adsorbers, incorporating them into PES membranes. The introduction of ZnO nanoparticles led to a notable enhancement in dye rejection capability. The rejection rate for methylene blue rose from 47.5% in reference PES membranes to 82.3% in the PES membranes blended with ZnO. The studies mentioned provide successful examples of application of various membrane fabrication techniques in developing adsorber-incorporated membranes. These membranes exhibit remarkable adsorption capacities for different types of organic contaminants. Such findings highlight the potential of these innovative membrane systems to remove specific pollutants effectively and sustainably from water.

The aim of this study was to create composite PES microfiltration membranes by incorporating adsorber polymer microparticles into the membrane structure, enabling the efficient removal of diverse EDCs from water. The adsorber polymer microparticles were synthesized using precipitation polymerization. To create the composite membranes, the adsorber polymer particles were mixed into the membrane dope solution and subsequently processed into flat sheet membranes. The synthesized adsorber polymer particles were immobilized in the porous PES membrane matrices by means of cross-linking using electron beam irradiation.[37] The electron beam irradiation technique at sufficient electron energy can effectively traverse the complete cross-section of the membrane. Consequently, in-depth, and thorough modifications become possible, expanding the range and extent of alterations to the membrane structure. This achievement occurs without relying on hazardous polymerization initiators or other toxic reagents.[38] Thus, this modification technique stands as an environmentally friendly choice. To evaluate the effectiveness of the developed composite membranes, a group of eight EDCs with varying physiochemical properties was chosen as the target adsorbates. These specific EDCs were chosen due to their widespread occurrence in water sources, their significant toxicity and endocrine disrupting properties. To assess the adsorption performance of the composite membranes, dynamic adsorption experiments were performed. During these experiments, the adsorption loading of both the composite membranes and the reference membranes (pristine membranes without adsorber particles) was measured and compared. To comprehensively investigate the characteristics and performance of both the pristine and composite PES membranes, a range of analytical techniques were employed. Water contact angle measurements and water permeance analysis were conducted to assess the

performance of the membranes in terms of hydrophilicity and flux, respectively. Moreover, scanning electron microscopy (SEM) and X-ray photoelectron spectroscopy (XPS) were performed to gain insights into the morphology and surface chemistry of the membranes. These characterizations provided valuable information regarding the structural and chemical properties of the membranes. Furthermore, a straightforward regeneration procedure was developed to allow for multiple reuses of the membranes while preserving their adsorption capacity.

Experimental

Materials and methods

Estrone (E1), 17β-estradiol (E2), ethinyl estradiol (EE2), estriole (E3), equiline (EQ), bisphenol A (BPA), androst-4-ene-3,17-dione (A4), testosterone (TST), acetonitrile (ACN), methacrylic acid (MAA), divinylbenzene (DVB), 1-methyl-2-pyrrolidone (NMP), and 2,2′-azobis (2-methylpropionitrile) (AIBN) were obtained from Sigma Aldrich (St. Louis, USA). Polyethylene glycol 400 (PEG) was purchased from Acros Organics, part of Thermo Fisher Scientific (Geel, Belgium). Absolute ethanol and toluene were purchased from VWR (Radnor, USA). Polyethersulfone (PES, Ultrason E2010) was provided by BASF, Ludwigshafen, Germany. A Milli-Q water purification system was utilized to generate ultra-pure water.

Preparation of adsorber particles

The adsorber polymer particles were synthesized by precipitation polymerization, a technique adapted from Celiz *et al.*[39] Initially, 8 mmol of methacrylic acid (MAA) were mixed with 40 mmol of divinylbenzene (DVB) and sonicated for 5 min. The resulting mixture was dissolved in a solution consisting of 60 mL of acetonitrile and toluene (3 : 1, v/v). It was further sonicated for 15 min to ensure a uniform solution. Next, the mixture was degassed by gently flowing nitrogen through it for 20 min and then sealed in a nitrogen environment. AIBN (2 wt% of MAA and DVB) was mixed with 2 mL of acetonitrile and added to the mixture *via* injection. The resulting mixture was stirred at 200 rpm using a mechanical stirrer and placed in a silicone oil bath at the temperature of 70 °C. After 2 h, the polymerization process was terminated by venting the system with air. The resulting particles were allowed to precipitate and subsequently washed three times with ethanol to remove any remaining monomers. Finally, the particles were left to dry at room temperature.

Preparation of the composite membranes

Flat sheet composite PES (C-PES) microfiltration membranes were synthesized through non-solvent induced phase separation (NIPS).[40] The polymer membrane dope solution (65 wt% PEG, 21 wt% NMP and 14 wt% PES) was mixed with the synthesized DVB polymer particles (4 wt% of the total polymer solution).[33] The mixing process was conducted for 0.5 h at a speed of 3500 rpm employing a mixer (SpeedMixer DAC 150.1 FVZ-K, Hauschild engineering, Hamm, Germany) until a uniform mixture was attained. The membrane polymer solution was subsequently deposited on a glass plate (200 μm gap casting knife). The polymer film was moved to a humidified chamber at room temperature for a duration of 5 min. Subsequently, the glass plate was immersed in a coagulation bath containing cooled ultrapure water (approximately 10 °C) for 5 min. Following this step, all membranes underwent a thorough rinsing with ultrapure water. During the phase inversion process, the adsorber DVB particles, (not soluble in both NMP or water), were effectively integrated in the PES membrane scaffold. In order to covalently immobilize the DVB polymer particles in the membrane structure, the fabricated membranes were exposed to electron beam irradiation while they were in a wet state. This irradiation was carried out using a custom-made electron accelerator at a dose rate of 150 kGy. This process took place in an N_2 atmosphere with O_2 quantities lower than 10 mg L^{-1}. Subsequently, all membranes were left to dry at room temperature. A reference PES membrane was prepared using the same procedure, excluding the incorporation of additional particles.

Characterization

Water permeability. The assessment of permeation rate involved measuring the time needed for 100 mL of pure water to pass though the membrane under a consistent pressure of 0.5 bar. A stainless-steel filtration cell (16249, Sartorius Stedim Biotech, Göttingen, Germany) was utilized for these permeation experiments. Each experiment was repeated three times, and the average value was calculated. The water permeation J (L h^{-1} m^{-2} bar^{-1}) was determined using eqn (1).

$$J = \frac{V}{t \times A \times p} \quad (1)$$

where V (L) represents the volume of the deionized water that was filtered, t (h) indicates the time taken for the filtration experiment, A (m^2) denotes the surface area of the tested membrane that was exposed during the filtration and p (bar) is the applied pressure.

Water contact angle. The water wettability as an indicator of hydrophilicity of both the pristine and composite PES membranes was assessed using a static contact angle measurement system (DSA 30E, Krüss, Hamburg, Germany) and the sessile drop method. In this method, a 5 μL droplet of deionized water was carefully placed on the surface of each membrane, and the contact angle formed by the droplet on the membrane was measured. To ensure reliable data, measurements were taken at five different locations on each membrane, and the results were averaged to obtain representative values.

XPS. The chemical composition of the upper surface region of both pristine and the synthesized composite PES membranes were examined using X-ray photoelectron spectroscopy (XPS) analysis (Kratos Axis Ultra instrument from Kratos Analytical Ltd, located in Manchester, UK).

SEM. The surface and cross-sectional morphologies of both pristine and composite membranes were examined using scanning electron microscopy (SEM) on an Ultra 55 SEM instrument (Carl Zeiss Ltd, Goettingen, Germany) at a range of

magnifications (from 10 000 to 25 000 times). To mitigate any charging effects during imaging, the membranes were coated with chromium layer (30 nm-Z400 sputter system, Leybold in Hanau, Germany).

To investigate the morphologies of the synthesized particles, a suspension of the particles in ethanol was applied to a silicon wafer, and the ethanol was left to evaporate at room temperature. Subsequently the morphology and size of the particles were analyzed using an Ultra 55 SEM instrument (Carl Zeiss Ltd, Göttingen, Germany), with a magnification ranging from 1000 to 10 000 times.

Batch adsorption test. The adsorption capacity of the synthesized polymer particles were determined through a batch experiment. Specifically, 10 mg of the synthesized DVB particles were added to 15 mL of 17β-estradiol (E2) solution in a 15 mL falcon tube with various initial concentrations. The adsorption capacity was measured over a range of time intervals, spanning from 5 minutes to 240 minutes using eqn (2).

$$\text{Adsorption capacity} = \frac{C_0 - C_f}{C_0} \times 100 \quad (2)$$

C_0 (mg L^{-1}) represents the initial concentration of E2 in the solution, while C_f (mg L^{-1}) denotes the concentration of E2 in the solution at the time of the measurement, which is the final concentration.

Dynamic adsorption tests. The dynamic adsorption capacities (Q_{dyn}) of the synthesized composite PES membrane and the pristine PES membrane were analyzed using a bench scale dead-end filtration system (16249, Sartorius Stedim Biotech, Göttingen, Germany). A 47 mm membrane disk was positioned

Table 1 Characteristics of selected EDCs

	Molar weight/ g mol^{-1}	Water solubility/ mg L^{-1} [41–43]	Log K_{ow} [41–43]	pK_a [41–43]	Detection setting (fluorescence excitation–emission or UV absorption/nm)	Structure
Estrone (E1) (metabolite of E2)	270.4	30	3.13	10.8	273–305	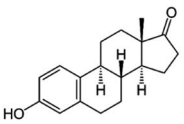
17β-Estradiol (E2) (natural hormone)	272.4	3.6	4.01	10.1	273–305	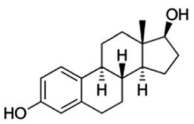
Ethinylestradiol (EE2) (ovulation inhibitor)	296.4	10	3.67	10.5	273–305	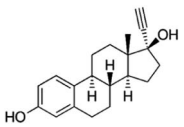
Estriol (E3) (natural hormone)	288.4	30	2.45	10.5	262–290	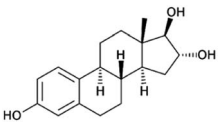
Equilin (EQ) (estrogen replacement)	268.3	1.4	3.35	9.4	280–310	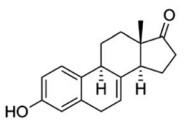
Testosterone (TST) (natural hormone)	288.4	23	3.32	18.5	246	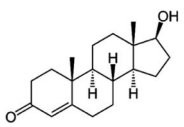
Androst-4-ene-3,17-dione (A4) (natural hormone)	286.4	57	2.72	14.5	246	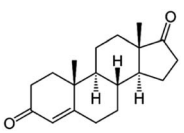
Bisphenol A (BPA) (plasticizer)	228.3	300	3.32	9.6–10.2	276–306	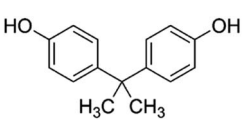

on the filter holder and wetted by flushing 25 mL of a water/ethanol (9 : 1, v/v) solution through the membrane before initiating the filtration process. EDC solutions were prepared with an initial concentration (C_0) of 5 mg L^{-1} in a water/ethanol mixture (9 : 1, v/v). Table 1 provides information on the properties of the tested EDCs, including their chemical structure, solubility, the octanol/water partition coefficient ($\log K_{ow}$), and the detection mode utilized for the measurement.[41–43] 60 mL of each EDC solution was passed through either the composite or pristine membrane under a constant pressure of 30 mbar. Permeate samples were collected at intervals of 1–10 mL. The concentrations of EDC in the permeate were measured using either fluorescent detection or UV absorption techniques (Infinite M200, Tecan, Germany).

Following each adsorption cycle, the membrane was rinsed by passing 20 mL of a water/ethanol solution (1 : 1, v/v) through it, followed by an additional 20 mL of a diluted water/ethanol solution (9 : 1, v/v). This washing procedure was repeated twice, resulting in a total of three adsorption cycles. The dynamic adsorption capacity (mg m^{-2}) was calculated using eqn (3).

$$Q_{dyn} = \frac{m_{ads}}{A_{membrane}} \quad (3)$$

The adsorbed amount of each EDC molecule, denoted as m_{ads} (mg), was determined by performing numerical analysis on the breakthrough (BT) curve data points in each adsorption cycle using OriginPro 2019b software from OriginLab. The active surface area of the membranes is represented by A (m^2).

To evaluate the effectiveness of the synthesized membranes in increasing adsorption loadings compared to the reference pristine membrane, the enhancement factor EF was calculated using the following equation:

$$EF = \frac{Q_{dyn\text{-}CPES}}{Q_{dyn\text{-}PES}} \quad (4)$$

where $Q_{dyn\text{-}CPES}$ (mg m^{-2}) is the average adsorption loading of the composite membrane over three adsorption cycles and $Q_{dyn\text{-}PES}$ (mg m^{-2}) is the average adsorption loading on the pristine PES membrane over three adsorption cycles. An EF value greater than 1 indicates an improvement in the adsorption capacity of the synthesized composite membrane compared to the reference pristine membrane.

Results and discussion

Membrane characterization

Morphology. In the present study, a comprehensive examination of the morphology and structure of DVB adsorber polymer particles, as well as the reference and composite membranes was conducted using SEM. Fig. 1a illustrates the structural characteristics of the particles under investigation. The observations reveal that the adsorber particles exhibit a spherical shape with an average size of 1.8 ± 0.4 μm. The particles display a smooth surface and remarkable uniformity in terms of size and shape. Furthermore, Fig. 1b indicates that

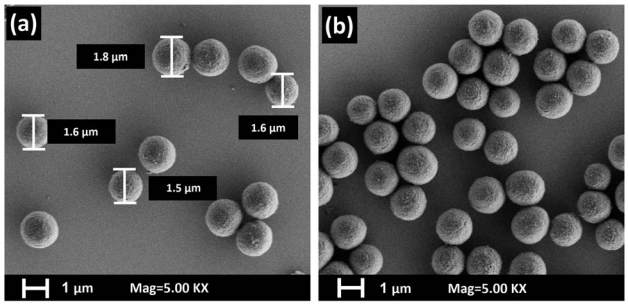

Fig. 1 (a) and (b). SEM images of divinyl benzene (DVB) particles.

the particles are densely packed and exhibit no signs of agglomeration, implying a high degree of stability and homogeneity in the material.

A comprehensive analysis of the surface and cross-sectional morphology and structure of both the pristine and composite PES membranes loaded with DVB polymer particles was carried out using SEM. The SEM micrographs presented in Fig. 2a and b demonstrate that the pristine PES membrane features a symmetric open pore structure. In contrast, Fig. 2c and d display that DVB polymer particles are uniformly distributed within the cross-section and pores of the composite membranes. The DVB polymer particles within the membrane pores are readily accessible, and there were no significant gaps formed within the membranes. Furthermore, the SEM images show no particle agglomeration within the membrane structure. However, some cavity structures were observed on the exterior surface of the composite membranes. This occurrence is probably a result of particles migrating into the water phase

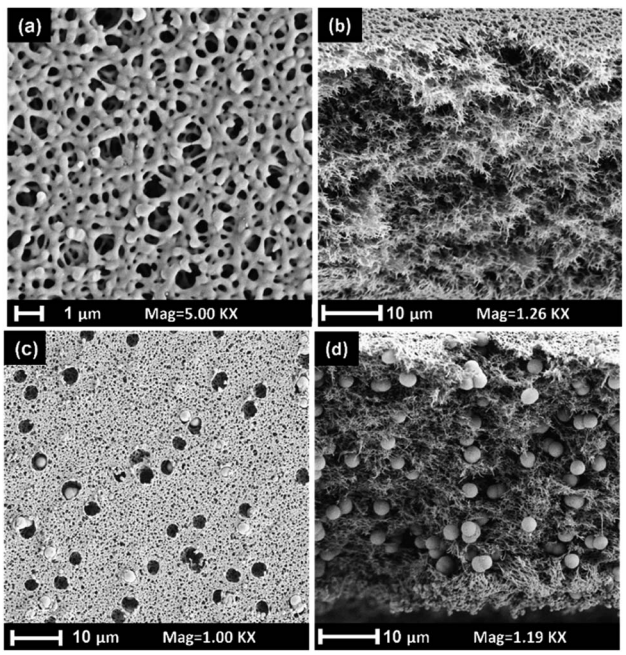

Fig. 2 SEM images of the (a) and (b) top surface and cross-section of the pristine PES membrane and (c) and (d) top surface and cross-section of the composite PES membranes.

Table 2 Water contact angle, water permeation, and chemical composition of the pristine and composite PES membranes

Membrane	WCA/°	Permeation/L h^{-1} m^{-2} bar^{-1}	Chemical composition/% C	O	S
PES	46 ± 4	14 500 ± 1000	75.7	18.4	5.9
C-PES	38 ± 2	12 500 ± 1200	75.4	18.3	6.3

during the phase-inversion process. These findings indicate that the composite membrane fabrication process has successfully loaded the DVB polymer particles onto the PES membrane matrix, providing a promising strategy for enhancing membrane performance.

Permeation, hydrophilicity, and chemical composition. The alteration in the membrane performance in terms of flux was investigated by conducting water permeance measurements. The results indicated that the reference PES membrane displayed a permeance of 14 500 ± 1000 L h^{-1} m^{-2} bar^{-1}, while the composite membrane exhibited slightly lower values. This slight decrease in the permeance can be ascribed to the particles present within the membrane structure, potentially causing partial blockage of certain pores. The analysis of WCA indicated that the pristine PES membrane was hydrophilic (WCA: 46° ± 4°). In contrast, the presence of the particles in the composite membrane surface led to a slight increase in wettability, resulting in a contact angle of 38° ± 2°. An optical image of the WCA is provided in Fig. 1s.† This improvement in the hydrophilicity can be attributed to the surface cavities formed on the composite membranes, as the surface roughness and structure also impact the WCA measurements.

The incorporation of adsorber DVB polymer particles in the membrane structure did not change the chemical composition of the surface of the synthesized composite membranes as confirmed by XPS measurements. Both membranes displayed similar chemical compositions, consisting of approximately 75% carbon (C), 18% oxygen (O), and 6% sulfur (S). Table 2 provides a comprehensive overview of the all the characterizations carried out.

Batch adsorption experiments. Batch adsorption experiments were carried out to assess the adsorption capacity of the synthesized DVB particles. Fig. 3 presents the adsorption capacity of these particles over varying time intervals (Fig. 3a) and across different initial concentrations of E2 after 30 min (Fig. 3b). The DVB polymer particles exhibit rapid kinetics for the removal of E2 from water. In the initial adsorption test performed after 5 min, 10 mg of DVB particles remove nearly 90% of E2 from the solution with an initial concentration of 10 mg L^{-1} (corresponding to an adsorption loading of 13.5 mg g^{-1}). As shown in Fig. 3b, when the initial concentration of the E2 solution is increased, the adsorption capacity of the 10 mg of DVB particles also increases until it reaches a plateau where further adsorption is likely impeded by particle saturation.

Song *et al.*[44] conducted a study on removing micropollutants from water by creating PES particles coated with amino groups.

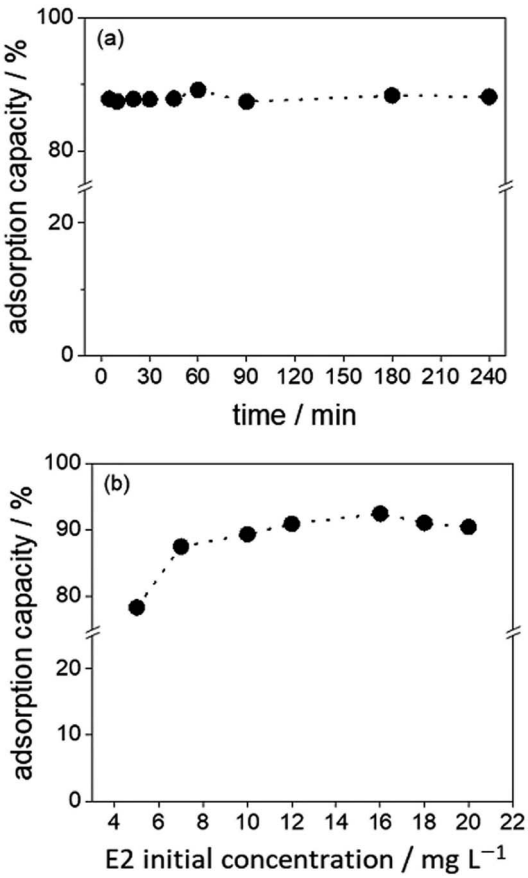

Fig. 3 Batch adsorption studies with DVB particles. (a) Adsorption capacities over time. (b) Adsorption capacity of DVB particles at different E2 initial concentrations.

They achieved this by applying amine groups to pre-existing PES particles. These amine-coated PES particles exhibited an adsorption loading of approximately 29 mg g^{-1}, it was reported that increasing the quantity of amino groups on the PES particles led to a significant increase in the adsorption loading of PES particles for the pollutant Congo red (CR). Enhancing the adsorption capacity of the DVB adsorber particles developed in this study can also be achieved by incorporating amino groups onto their surface.

Dynamic adsorption experiments. To evaluate membrane adsorption capacity, dynamic adsorption experiments were performed on both the reference PES membrane and the newly synthesized composite PES membranes. The experimental procedure involved three adsorption filtration cycles, with a washing step between each cycle. Breakthrough (BT) curves were obtained for each cycle, which provided information on the adsorption performance of the membranes. Fig. 4 presents the BT curves for the tested EDCs over three adsorption cycles. Table 3 summarizes the adsorption loading and adsorption capacity values over the three adsorption cycles. The results indicated that the C-PES membranes exhibited significantly higher adsorption capacities for all the tested EDCs compared to the reference pristine PES membrane. The C-PES membrane

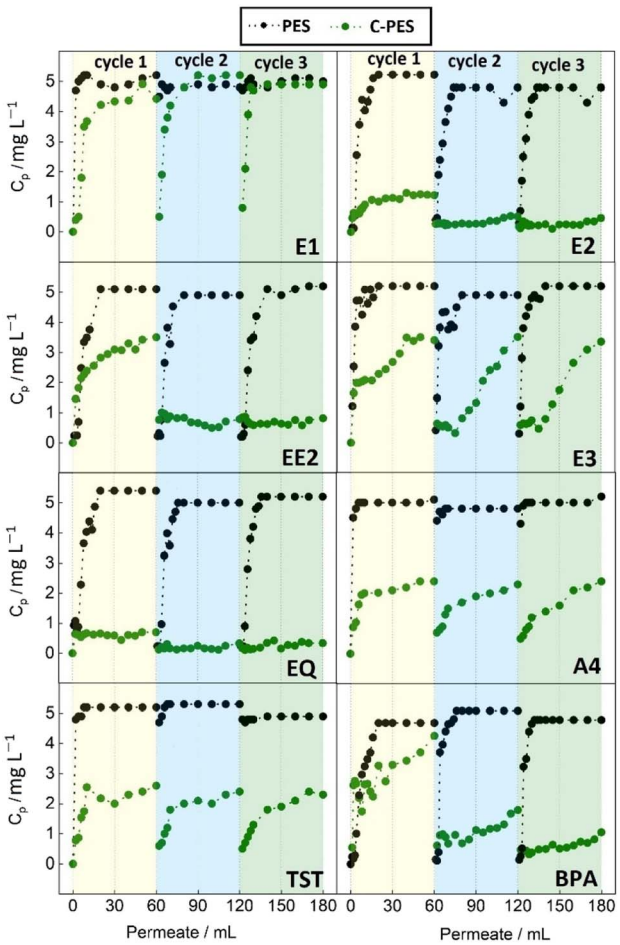

Fig. 4 Breakthrough (BT) curves for the reference pristine PES (black) and composite PES (green) membranes for filtering EDCs from water in three subsequent cycles with a regeneration step between each 60 mL of filtration.

exhibited an approximately fourfold higher adsorption capacity compared to the reference PES membrane for E1. Despite the increased adsorption capacity of the composite membrane, it is noteworthy that both the reference PES membrane and the composite PES membrane exhibited declining adsorption capacity in subsequent cycles of use. This decline suggests that the washing procedure employed to regenerate the membranes was not fully effective in removing the adsorbed E1 from the membrane.

In terms of adsorption capacity for E2, the composite membrane demonstrated notable performance advantage over the reference pristine PES membrane. The pristine PES membrane reached a saturation plateau after filtering 15 mL of the E2 solution, indicating limited adsorption capacity. In contrast, the C-PES membrane did not reach saturation even after filtration 60 mL of the solution, indicating a superior adsorption capacity. The composite membrane removed E2 at a rate approximately eight times higher than the reference membrane. Moreover, the adsorption capacity of the composite membrane increased in the subsequent cycles, with over 90% of the initial E2 being removed from the solution in both the second and third cycles. On the other hand, the adsorption capacity of the reference PES membrane declined in the subsequent cycles, indicating a limited capacity for E2 removal.

Both PES and C-PES membranes exhibited similar initial EE2 adsorption behavior to the adsorption of E2, with PES reaching saturation early, indicating limited capacity. In contrast, the composite membrane adsorbed over 50% of EE2, and with subsequent cycles, it improved to remove more than 80% of the initial EE2 from water.

The reference PES membrane had consistently low adsorption for E3, staying at an adsorption capacity of 7% of the initial E3 throughout all cycles. This suggests limited adsorption capacity. In contrast, the composite PES membranes significantly improved E3 adsorption. In the first cycle, over 50% of the initial E3 was removed from water, and this capacity continued to increase in subsequent cycles. By the third cycle, the composite membrane removed 66% of the initial E3, demonstrating enhanced performance and increasing adsorption capacity.

Regarding EQ, the reference PES membrane had limited adsorption effectiveness, removing only 13% of the initial EQ in the first cycle. In contrast, the composite membrane showed a significantly higher adsorption capacity. In the first cycle, it

Table 3 Dynamic adsorption loadings (mg m^{-2}) and adsorption capacity (%) of the reference pristine and composite PES membranes over three adsorption cycles

	Dynamic adsorption loading/mg m^{-2} (adsorption capacity/%)					
	PES			C-PES		
EDCs	Cycle 1	Cycle 2	Cycle 3	Cycle 1	Cycle 2	Cycle 3
E1	10 ± 1 (6%)	5 ± 1 (3%)	7 ± 1 (4%)	38 ± 4 (22%)	23 ± 2 (13%)	13 ± 1 (7%)
E2	15 ± 2 (8%)	18 ± 2 (11%)	14 ± 1 (8%)	128 ± 10 (77%)	158 ± 16 (93%)	157 ± 15 (95%)
EE2	25 ± 3 (14%)	20 ± 2 (12%)	28 ± 3 (15%)	94 ± 10 (48%)	155 ± 15 (86%)	150 ± 15 (86%)
E3	10 ± 1 (5%)	14 ± 2 (8%)	14 ± 2 (7%)	102 ± 10 (52%)	129 ± 13 (69%)	121 ± 12 (66%)
EQ	25 ± 3 (13%)	20 ± 2 (11%)	21 ± 2 (11%)	158 ± 16 (95%)	201 ± 20 (97%)	177 ± 18 (95%)
A4	7 ± 1 (4%)	4 ± 1 (2%)	7 ± 1 (4%)	95 ± 10 (57%)	111 ± 10 (64%)	122 ± 12 (68%)
TST	3 ± 1 (1%)	5 ± 1 (3%)	4 ± 1 (3%)	88 ± 9 (54%)	116 ± 11 (63%)	110 ± 11 (63%)
BPA	22 ± 2 (13%)	15 ± 1 (8%)	13 ± 1 (8%)	71 ± 7 (39%)	131 ± 13 (78%)	145 ± 15 (88%)

removed approximately 95% of the initial EQ, indicating a substantial improvement. Moreover, the composite membrane maintained this high EQ adsorption capacity in subsequent cycles, consistently removing around 95% of the initial EQ concentration, demonstrating stable and long-lasting adsorption capability.

For A4 adsorption, the reference PES membrane had low capacity, removing 4–7% of the initial A4 in each cycle, indicating limited effectiveness. Conversely, the composite PES membrane significantly improved A4 removal. In the first cycle, it removed 57% of the initial A4, and this capacity increased to 64% and 68% in the second and third cycles, highlighting its enhanced performance.

Regarding TST adsorption, the reference PES membrane had limited performance, removing only 3% of the initial TST in each cycle, suggesting low adsorption capacity. In contrast, the composite PES membrane showed significantly improved TST removal. In the first cycle, it removed 54% of the initial TST, and this capacity remained consistent in the second and third cycles, with TST removal rates of 63% for each cycle, indicating enhanced adsorption.

In the case of BPA, the reference PES membrane initially removed 13% of the initial BPA, with decreasing performance in subsequent cycles. Conversely, the C-PES membrane displayed significantly higher BPA adsorption. In the first cycle, it removed approximately 39% of the initial BPA, a notable improvement over the reference PES membrane. Furthermore, the composite membrane's adsorption capacity increased in the second and third cycles, removing approximately 78% and 88% of the initial BPA, respectively. This highlights the composite membrane's sustained high adsorption capacity and improved BPA adsorption performance in each cycle.

The BT curves obtained for the EDCs during the dynamic adsorption cycles indicate that the concentration of EDCs in the permeate increased gradually as the filtration volume increased. This suggests that the adsorption capacity of the membrane became saturated, leading to the breakthrough of the EDCs into the permeate. Moreover, the washing cycle performed between each adsorption cycle proved to be an effective method for regenerating the composite membranes. The composite membranes were able to maintain their adsorption capacity for up to three cycles without experiencing a substantial decline. This indicates that the washing procedure was successful in removing the adsorbed EDCs from the membrane surface, allowing for renewed adsorption capacity in subsequent cycles. In some cases (E2, EE2, BPA) an improvement was visible in between the first and second cycle. The retention of the tested EDCs is evidently attributed to adsorption effects since the pore size of the tested membranes is significantly larger, by several orders of magnitude, than the size of the EDC molecules. The significant increase in the adsorption capacity observed in the composite membranes can be attributed to the incorporation of the adsorber DVB particles. These particles have a high affinity for the EDCs, allowing for enhanced adsorption performance compared to the reference pristine PES membrane. The removal of EDCs by membranes involves a variety of mechanisms, including steric interaction, charge exclusion, and adsorption to the surface of the membrane. In this study, the eight EDCs under investigation are primarily in their undissociated form at the experimental pH value of 7, leading to minimal ionic interactions between the EDCs and the membranes. Moreover, the membrane's pore size is significantly larger than the size of the EDC molecules, making steric exclusion unlikely. Consequently, the main removal mechanism is expected to be adsorption, where EDC molecules adhere to the membrane surface. EDCs adsorption or partitioning to the membrane is mainly driven by hydrophobic interactions and hydrogen bonding. As indicated in Table 1, all the EDCs tested in this study exhibit hydrophobic characteristics. The DVB particles contribute to a larger surface area, providing numerous adsorption sites for the EDCs.

The adsorption mechanism of the EDC molecules onto the adsorber polymer particles involves a combination of physical and chemical interactions. Initially, weak van der Waals forces promote the initial attraction between EDCs and the surface of the adsorber particles.[45] As EDCs approach the particle surface, stronger adsorption takes place. The primary mechanism behind the adsorption of EDCs onto DVB particles is the π–π stacking interaction, stemming from the presence of aromatic rings on both the DVB and EDC molecules. When these aromatic rings come into close proximity, they can form π–π stacking complexes, creating a strong attractive force during the adsorption process.[46,47] Furthermore, this interaction can facilitate the formation of hydrogen bonds.[48] EDC molecules also have the potential to form hydrogen bonds with MAA present in the adsorber particles. Specifically, hydrogen bonds are formed between the hydrogen atom of the EDC molecule's hydroxyl group and the oxygen-containing functional groups within the adsorber particles.[49,50] These hydrogen bonds significantly enhance the overall adsorption of EDCs to the adsorber particles, thus improving the effectiveness of the adsorption process.

Additionally, EDCs with higher log K_{ow} values and lower water solubility are expected to be more easily removed from the water phase. The research findings suggest that the adsorption of hydrophobic EDCs is linked to their octanol–water partition coefficient. The analysis of the adsorption loading and the log K_{ow} and water solubility values (presented in Table 1), indicate that the unmodified PES membrane predominantly removes EDCs through hydrophobic interactions. Consequently, compounds with higher log K_{ow} and lower water solubility values exhibit greater adsorption, indicating a correlation between the hydrophobicity of the compound and its removal efficacy. The increase in the adsorption loading after the regeneration procedure can be due to the swelling of the membrane and particles with ethanol and increased the number of active surface sites for adsorption. The assessment of the adsorption efficiency of the composite membranes in relation to the pristine membrane was conducted using eqn (4). The findings presented in Fig. 5 indicated a substantial enhancement in the adsorption performance of the composite membranes. Notably amongst the tested EDCs, TST showed the most pronounced increase in the average adsorption loading compared to the pristine membrane, followed by A4 and E2. In contrast, E1 demonstrated the lowest enhancement factor. The incorporation of DVB particles within

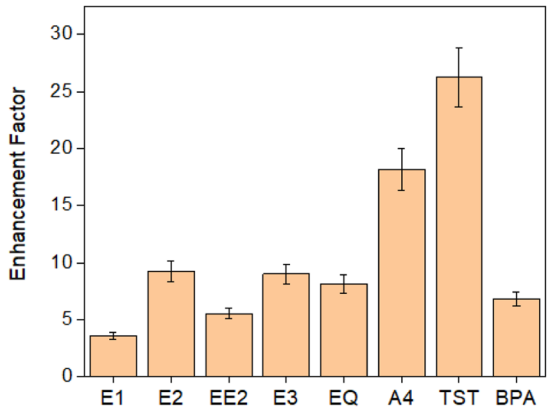

Fig. 5 Enhancement factor EF for the adsorption of the different EDCs.

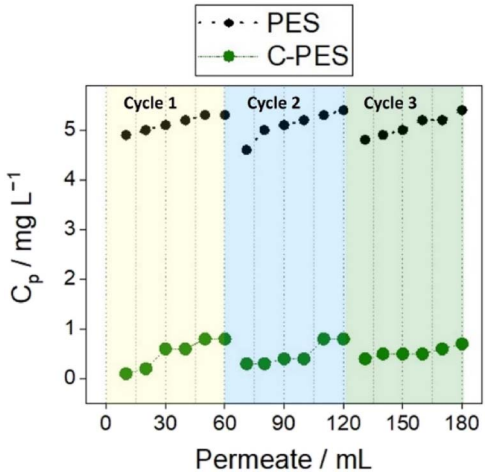

Fig. 6 Dynamic adsorption experiments conducted with E2 solutions prepared with tap water.

the PES membrane introduces additional surface area and active sites. This augmentation facilitates a greater degree of interaction between the membrane and the molecules of interest, consequently resulting in an increased adsorption capacity. Considering that the primary adsorption mechanisms likely revolve around π–π stacking and the formation of hydrogen bonds, it can be suggested that this system exhibits potential for removing a wide range of micropollutants, surpassing the realm of EDCs. Specifically, micropollutants with aromatic structures are prone to engaging in π–π stacking interactions, while those featuring hydrogen atoms on their hydroxyl groups can form hydrogen bonds in this system.

Zhang *et al.*[51] exhibited that the NF Desal-5 DK membrane displayed an adsorption capacity of 0.03 μg m^{-2} (computed from the provided data) for BPA during the dynamic filtration of a 200 mL BPA solution. The adsorption capacity of the membranes synthesized in our study surpasses this value reported for nanofiltration by three orders of magnitude. According to McCallum *et al.*,[52] the adsorption capacity of NF-270 membranes for E2 was 1.2 mg m^{-2} (derived from the data), which remains two orders of magnitude lower than the average adsorption capacity of our membranes. In a subsequent investigation by Semião *et al.*,[53] even lower values are recorded for the adsorption of E2 by NF-270 (0.008 mg m^{-2}, computed from the data). In research conducted by Guo *et al.*,[54] they immobilized silver nanoparticles onto the surface of a NF membrane that had been coated with dopamine. Although this modification led to a reduction of 4–10% in the membrane's already low permeability, the resulting composite membranes displayed a slight improvement in the rejection of BPA, rising from 98% to 99%. This enhancement was attributed to the improved size exclusion facilitated by the modified membrane structure. Kaminska *et al.*[55] integrated single-walled carbon nanotubes into PES membranes and investigated the removal and adsorption of BPA. The PES/nanocomposite membranes removed nearly 80% of the BPA from water (with an initial concentration of 0.001 mg L^{-1}), while the reference pristine membrane only managed to eliminate around 40% of the BPA. The permeation characteristics of the PES/nanocomposite membranes fell within the ultrafiltration range. This implies that the modification with our synthesized DVB microparticles offers a dual advantage: increased adsorption (BPA initial concentration was 5 mg L^{-1}), coupled with higher permeation.

Liao *et al.*[25] introduced hollow mesoporous carbon nanospheres into the PES UF membrane's pores. Their system demonstrated an impressive 94% removal of E2 under relatively low-pressure conditions of 0.15 bar, alongside a water flux of 64 L h^{-1} m^{-2}. In a separate investigation Nguyen *et al.*,[56] integrated single-walled carbon nanotubes (SWCNTs) into a PES UF membrane through mechanical means. In comparable operational settings, their system managed to achieve a 65% removal of E2, given an initial E2 concentration of 100 ng L^{-1}. In contrast to these studies, our composite membrane excelled in E2 removal, even when subjected to a notably higher initial concentration of 5 mg L^{-1}.

Real water application. This study assessed the performance of composite and reference PES membranes in removing EDCs from real water samples. A 5 mg L^{-1} E2 solution was prepared using tap water, and 60 mL of this solution was passed through the membranes to determine dynamic adsorption loading. This procedure was repeated three times with a washing step in between. The BT curves are illustrated in Fig. 6. The C-PES membrane exhibited an average dynamic adsorption loading of 161 mg m^{-2} throughout the three cycles, similar to when pure deionized water was used. The reference membrane showed a slightly lower dynamic adsorption loading with an average value of 11 mg m^{-2}. The results suggest that unlike the reference membrane, the composite membrane's adsorption capacity is unaffected by the presence of salts and organic matter in the tap water. The details on tap water composition is provided ESI Table 1s.†

Conclusion

Composite polyethersulfone (PES) membranes incorporated with adsorber polymeric divinyl benzene (DVB) particles were successfully prepared. The adsorber particles, prepared *via* precipitation polymerization, were covalently integrated into

the PES membranes using electron beam irradiation, a method known for being environmentally friendly and sustainable. The proposed modification allows for continuous water filtration while simultaneously facilitating the adsorption of endocrine disrupting chemicals (EDCs) from water. The dynamic adsorption experiments revealed the fabricated composite membranes achieved 95% removal of 17β-estradiol and 88% removal of bisphenol-A, all while maintaining a substantial water flux of 12 500 ± 1200 L h^{-1} m^{-2} bar^{-1}. This removal rate is approximately two orders of magnitude greater than that of the commercial NF membranes, which are additionally hindered by the limitation of lower water flux. Furthermore, the composite membranes synthesized in this study effectively removed testosterone, androst-4-ene-3,17-dione, estriol, ethinylestradiol, and equilin within the range of 63% to 97%. The remarkable adsorption performance of the synthesized composite membranes can be attributed to factors such as an expanded surface area available for adsorption and the hydrophobic nature of the EDCs. Moreover, the composite membranes can be rapidly regenerated, indicating their potential for effective reusability and alignment with the requirements of sustainable processes. Overall, the potential of incorporating polymeric adsorber particles into porous polymer membranes through electron beam irradiation has been successfully established. Due to their remarkable adsorption capacity, ability to maintain high water permeability even under low pressure, and ease of regeneration, the composite membranes synthesized in this study have the potential to serve as efficient filters for rapid potable water purification, presenting significant commercial possibilities.

Author contributions

Zahra Niavarani: methodology, investigation, data curation, writing original draft, writing – review, and editing. Daniel Breite: writing – review, and editing, supervision. Berfu Ulutaş: investigation. Andrea Prager: SEM and XPS measurements. Ömer Kantoğlu: writing – review and editing, supervision. Bernd Abel: writing – review and editing, supervision. Roger Gläser: writing – review and editing, supervision. Agnes Schulze: writing – review and editing, supervision.

Conflicts of interest

There are no conflicts to declare.

References

1 C. D. Metcalfe, S. Bayen, M. Desrosiers, G. Muñoz, S. Sauvé and V. Yargeau, *Environ. Res.*, 2022, **207**, 112658.
2 C. Pironti, M. Ricciardi, A. Proto, P. M. Bianco, L. Montano and O. Motta, *Water*, 2021, **13**, 1347.
3 B. Yilmaz, H. Terekeci, S. Sandal and F. Kelestimur, *Rev. Endocr. Metab. Disord.*, 2020, **21**, 127–147.
4 W. Rodprasert, J. Toppari and H. E. Virtanen, *Front. Endocrinol.*, 2021, **12**, 706532.
5 J. D. Meeker, *Am. J. Dis. Child.*, 2012, **166**, 952–958.
6 V. L. Marlatt, S. Bayen, D. Castaneda-Cortès, G. Delbès, P. Grigorova, V. S. Langlois, C. J. Martyniuk, C. D. Metcalfe, L. Parent, A. Rwigemera, P. Thomson and G. Van Der Kraak, *Environ. Res.*, 2022, **208**, 112584.
7 F. M. Windsor, S. J. Ormerod and C. R. Tyler, *Biol. Rev.*, 2018, **93**, 626–641.
8 M. F. M. A. Zamri, R. Bahru, F. Suja, A. H. Shamsuddin, S. K. Pramanik and I. M. R. Fattah, *J. Water Process. Eng.*, 2021, **41**, 102017.
9 P. Rajasulochana and V. Preethy, *Resour.-Effic. Technol.*, 2016, **2**, 175–184.
10 R. Mailler, J. Gasperi, Y. Coquet, A. Buleté, E. Vulliet, S. Deshayes, S. Zedek, C. Mirande-Bret, V. Eudes, A. Bressy, E. Caupos, R. Moilleron, G. Chebbo and V. Rocher, *Sci. Total Environ.*, 2016, **542**, 983–996.
11 J. L. Bennett, A. L. Mackie, Y. Park and G. A. Gagnon, *Aquacult. Eng.*, 2018, **83**, 40–46.
12 M. Mustafa, I. Kozyatnyk, C. Gallampois, P. Oesterle, M. Östman and M. Tysklind, *Sci. Total Environ.*, 2021, **776**, 145723.
13 H.-S. Park, J. R. Koduru, K.-H. Choo and B. Lee, *J. Hazard. Mater.*, 2015, **286**, 315–324.
14 E. Gagliano, M. Sgroi, P. P. Falciglia, F. G. A. Vagliasindi and P. Roccaro, *Water Res.*, 2020, **171**, 115381.
15 P. Márquez, A. Benítez, A. F. Chica, M. A. Martín and A. Caballero, *J. Cleaner Prod.*, 2022, **366**, 132685.
16 D. Azizi, A. Arif, D. Blair, J. Dionne, Y. Filion, Y. Ouarda, A. G. Pazmino, R. Pulicharla, V. Rilstone, B. Tiwari, L. Vignale, S. K. Brar, P. Champagne, P. Drogui, V. S. Langlois and J.-F. Blais, *Environ. Res.*, 2022, **207**, 112196.
17 P. Xu, C. Bellona and J. E. Drewes, *J. Membr. Sci.*, 2010, **353**, 111–121.
18 M. Hafiz, A. H. Hawari, R. Alfahel, M. K. Hassan and A. Altaee, *Membranes*, 2021, **11**, 32.
19 A. F. S. Foureaux, E. O. Reis, Y. Lebron, V. Moreira, L. V. Santos, M. S. Amaral and L. C. Lange, *Sep. Purif. Technol.*, 2019, **212**, 171–179.
20 J. Radjenović, M. Petrović, F. Ventura and D. Barceló, *Water Res.*, 2008, **42**, 3601–3610.
21 Z. Niavarani, D. Breite, A. Prager, B. Abel and A. Schulze, *Membranes*, 2021, **11**(2), 99.
22 S. Uebele, T. Goetz, M. Ulbricht and T. Schiestel, *ACS Appl. Polym. Mater.*, 2022, **4**, 1705–1716.
23 K. Niedergall, M. Bach, T. Schiestel and G. E. M. Tovar, *Ind. Eng. Chem. Res.*, 2013, **52**, 14011–14018.
24 J. Kuttiani Ali, M. Abi Jaoude and E. Alhseinat, *Sep. Purif. Technol.*, 2021, **266**, 118585.
25 Z. Liao, M. N. Nguyen, G. Wan, J. Xie, L. Ni, J. Qi, J. Li and A. I. Schäfer, *J. Hazard. Mater.*, 2020, **397**, 122779.
26 N. A. Ahmad, P. S. Goh, N. Azman, A. F. Ismail, H. Hasbullah, N. Hashim, N. D. Kerisnan@Krishnan, N. K. E. M. Yahaya, A. Mohamed, M. A. Mohamed Yusoff, J. Karim and N. S. Abdullah, *Membranes*, 2022, **12**, 958.
27 V. Vatanpour, S. S. Madaeni, R. Moradian, S. Zinadini and B. Astinchap, *J. Membr. Sci.*, 2011, **375**, 284–294.
28 H. Wu, B. Tang and P. Wu, *J. Membr. Sci.*, 2013, **428**, 341–348.

29 H. Joo Kim, H. Raj Pant, J. Hee Kim, N. Jung Choi and C. Sang Kim, *Ceram. Int.*, 2014, **40**, 3023–3029.
30 A. Tiraferri, C. D. Vecitis and M. Elimelech, *ACS Appl. Mater. Interfaces*, 2011, **3**, 2869–2877.
31 M. Tagliavini and A. I. Schäfer, *J. Hazard. Mater.*, 2018, **353**, 514–521.
32 L. Roshanfekr Rad and M. Anbia, *J. Environ. Chem. Eng.*, 2021, **9**, 106088.
33 Z. Niavarani, D. Breite, A. Prager, I. Thomas, M. Kuehnert, B. Abel, R. Gläser and A. Schulze, *Mater. Chem. Front.*, 2023, **7**(19), 4460–4472.
34 K. Niedergall, M. Bach, T. Hirth, G. E. M. Tovar and T. Schiestel, *Sep. Purif. Technol.*, 2014, **131**, 60–68.
35 S. Lotfi, K. Fischer, A. Schulze and A. I. Schäfer, *Nat. Nanotechnol.*, 2022, **17**, 417–423.
36 S. Balta, A. Sotto, P. Luis, L. Benea, B. Van der Bruggen and J. Kim, *J. Membr. Sci.*, 2012, **389**, 155–161.
37 M. Schmidt, S. Zahn, F. Gehlhaar, A. Prager, J. Griebel, A. Kahnt, W. Knolle, R. Konieczny, R. Gläser and A. Schulze, *Polymers*, 2021, **13**(11), 1849.
38 R. Das, M. Kuehnert, A. Sadat Kazemi, Y. Abdi and A. Schulze, *Polymers*, 2019, **11**, 344.
39 M. D. Celiz, D. S. Aga and L. A. Colón, *Microchem. J.*, 2009, **92**, 174–179.
40 D. Breite, M. Went, I. Thomas, A. Prager and A. Schulze, *RSC Adv.*, 2016, **6**, 65383–65391.
41 Y. Yoon, P. Westerhoff, S. A. Snyder, E. C. Wert and J. Yoon, *Desalination*, 2007, **202**, 16–23.
42 A. M. Comerton, R. C. Andrews, D. M. Bagley and P. Yang, *J. Membr. Sci.*, 2007, **303**, 267–277.
43 I. Kim, Z. Yu, B. Xiao and W. Huang, *Environ. Toxicol. Chem.*, 2007, **26**, 264–270.
44 X. Song, R. Wang, W. Zhao, S. Sun and C. Zhao, *J. Colloid Interface Sci.*, 2017, **485**, 39–50.
45 S. Beyazit, B. Tse Sum Bui, K. Haupt and C. Gonzato, *Prog. Polym. Sci.*, 2016, **62**, 1–21.
46 Y. Gong, Z. Chen, L. Bi, J. Kang, X. Zhang, S. Zhao, Y. Wu, Y. Tong and J. Shen, *Sci. Total Environ.*, 2021, **781**, 146635.
47 H. T. Nguyen, N. T. Vuong Bui, W. G. Kanhounnon, K. L. Vu Huynh, T.-V.-A. Nguyen, H. M. Nguyen, M. H. Do, M. Badawi and U. D. Thach, *RSC Adv.*, 2021, **11**, 34281–34290.
48 R. Istratie, R. Băbuță, A. Popa, C. Păcurariu and M. Stoia, *Water, Air, Soil Pollut.*, 2017, **228**, 276.
49 J. Zhang, M. N. Nguyen, Y. Li, C. Yang and A. I. Schäfer, *J. Hazard. Mater.*, 2020, **391**, 122020.
50 X. Liu, Y. Zhang, H. Ju, F. Yang, X. Luo and L. Zhang, *Colloids Surf., A*, 2021, **629**, 127424.
51 Y. Zhang, C. Causserand, P. Aimar and J. P. Cravedi, *Water Res.*, 2006, **40**, 3793–3799.
52 E. A. McCallum, H. Hyung, T. A. Do, C.-H. Huang and J.-H. Kim, *J. Membr. Sci.*, 2008, **319**, 38–43.
53 A. J. C. Semião and A. I. Schäfer, *J. Membr. Sci.*, 2011, **381**, 132–141.
54 H. Guo, Y. Deng, Z. Yao, Z. Yang, J. Wang, C. Lin, T. Zhang, B. Zhu and C. Y. Tang, *Water Res.*, 2017, **121**, 197–203.
55 G. Kaminska, J. Bohdziewicz, J. I. Calvo, P. Prádanos, L. Palacio and A. Hernández, *J. Membr. Sci.*, 2015, **493**, 66–79.
56 M. N. Nguyen, P. B. Trinh, C. J. Burkhardt and A. I. Schäfer, *Sep. Purif. Technol.*, 2021, **264**, 118405.